

This is the accepted manuscript made available via CHORUS. The article has been published as:

# Hyperferroelectricity in ZnO: Evidence from analytic formulation and numerical calculations

Rajendra Adhikari and Huaxiang Fu

Phys. Rev. B **99**, 104101 — Published 4 March 2019

DOI: [10.1103/PhysRevB.99.104101](https://doi.org/10.1103/PhysRevB.99.104101)

# Hyperferroelectricity in ZnO: Various evidence from analytic formulation and numerical calculations

Rajendra Adhikari<sup>1,2</sup> and Huaxiang Fu<sup>1</sup>

<sup>1</sup> *Department of Physics, University of Arkansas, Fayetteville, Arkansas 72701, USA*

<sup>2</sup> *Department of Natural Sciences, Kathmandu University, Dhulikhel, Kavre, Nepal*

(Dated: January 28, 2019)

Hyperferroelectricity is an interesting phenomenon. Hexagonal ABC-type semiconductor LiZnAs was discovered to be hyperferroelectric (HyFE) [Garrity, Rabe, and Vanderbilt, Phys. Rev. Lett. 112, 127601 (2014)]. ZnO is a technologically important semiconductor and possesses a wurtzite crystal structure similar to LiZnAs. It raises an intriguing question whether ZnO is HyFE. Here we use various approaches to address this question of importance, by determining the electric equation of state, the free energy of ZnO under an open-circuit boundary condition (OCBC), as well as the vibration properties of LO phonon. We find (i) The  $D \sim \lambda$  curve of ZnO, where  $D$  is electric displacement and  $\lambda = P/0.844$  is a parameter directly proportional to polarization  $P$ , exhibits one and only one root at  $\lambda=0$ ; (ii) Under OCBC, the free energy of ZnO does not produce a minimum at structural phase of nonzero polarization; (iii) The longitudinal optic (LO) phonon with computed frequency  $\omega_{LO}=255 \text{ cm}^{-1}$  in centrosymmetric ZnO is not soft and does not have an imaginary frequency. These results corroborate the others and consistently lead to the conclusion that, although ZnO is interestingly on the edge of becoming a HyFE, it is not yet a HyFE. We further provide a physical origin explaining why ZnO is not HyFE, and reveal a possibility that may turn ZnO into a HyFE.

## I. INTRODUCTION

Hyperferroelectricity, in which a *proper* ferroelectric solid of spontaneous polarization maintains its ferroelectricity under an open-circuit boundary condition (OCBC), is an interesting phenomenon of fundamental and technological relevance.<sup>1,2</sup> Fundamentally, unlike in improper ferroelectrics<sup>3-6</sup>, the open-circuit boundary condition often generates a strong depolarization field in proper ferroelectrics, which tends to eliminate utterly the ferroelectricity and polarization.<sup>7,8</sup> It is therefore profoundly interesting to understand the physics behind hyperferroelectricity, and to investigate why ferroelectricity and atomic off-center displacements persist in hyperferroelectrics (HyFE), defying the existence of strong depolarization fields. Possible explanations thus far include small LO/TO splitting<sup>1</sup>, competition between well depth and spontaneous polarization<sup>9</sup>, instability driven by short-range interaction<sup>10</sup>, and meta-screening<sup>11</sup>. Furthermore, determination of the free energy when a HyFE is under OCBC, and determination of the electric equation of state for a HyFE, are topics of fundamental importance. These knowledge may also help in the future search and design of new hyperferroelectric solids. Technologically, HyFE can be used to form interfaces with other functional materials such as semiconductors, topological insulators, and ferromagnetics, where a nonzero polarization maintained in HyFE can effectively tune, control, and enhance the properties of the functional materials. Furthermore, certain hyperferroelectrics were shown to have negative longitudinal piezoelectric coefficients.<sup>12</sup> To take advantage of the unusual properties of hyperferroelectricity, determining and understanding whether a solid is HyFE is the key.

HyFE was discovered recently in hexagonal ABC-type

semiconductors such as LiBeSb and LiZnAs.<sup>1</sup> LiZnAs (and LiBeSb) have a crystal structure similar to the wurtzite semiconductors, in the sense that Zn and As occupy the atomic sites of the wurtzite lattice. Furthermore, both Zn and As atoms form tetrahedral bonds with its neighbors. The minor difference in LiZnAs, compared to the wurtzite structure, is the existence of stuffing Li atoms which are located between the atomic layers in wurtzite structure. Based on the marked resemblance between ABC-type and wurtzite semiconductors, it is intriguing to determine whether wurtzite semiconductor ZnO is a HyFE, and to investigate the underlying physics and mechanism behind the conclusion.

ZnO is a polar semiconductor of technological importance<sup>13</sup>. Being polar, ZnO offers an interesting possibility of utilizing its polarization to control the already-appealing electronic properties, forming so-called polarization electronics. Also, ZnO has an exceptionally large exciton binding energy of  $\sim 60 \text{ meV}$ , suitable for fabricating microelectronics and optical devices that may operate at high temperatures under extreme environments.<sup>14</sup> Meanwhile, ZnO exhibits a large piezoelectric coefficient<sup>15</sup>, which makes it an excellent candidate for piezoelectric semiconductor. ZnO also possesses the largest electromechanical  $d_{33}$  coefficient among the wurtzite semiconductors<sup>16</sup>, and its  $d_{33} = 12.4 \text{ pC/N}$  value is much larger than the  $d_{33} = 1.58 \text{ pC/N}$  value in GaN.<sup>17</sup> The large  $d_{33}$  coefficient in ZnO originates from the local-polarization rotation mechanism<sup>16</sup>, similar to what occurs in ferroelectric solids<sup>18-20</sup>. Moreover, after doping, ZnO shows high electrical conductivity and serves as a good transparent conductor.<sup>21-23</sup>

The purpose of this paper is to formulate and use various approaches to determine whether ZnO is HyFE, and to reveal important physics on what characteristic prop-

erties a HyFE should have. The various approaches include (i) the determination of the electric equation of state, which yields the relationship between electric displacement ( $\vec{D}$ ) and polarization ( $\vec{P}$ ); (ii) the determination of free energy under OCBC with a vanishing electric displacement ( $\vec{D}=0$ ); (iii) the calculation of longitudinal optic phonon, which reveals lattice stability under the open-circuit boundary condition. These formulated methods are rather general and can be applied to solids other than ZnO. We find that different methods lead to a consensus conclusion, that is, although ZnO is interestingly on the edge of becoming a HyFE, it is not HyFE. We further provide a physical origin that explains why ZnO is not yet a HyFE, and reveal possible condition under which ZnO may become a HyFE.

## II. THEORETICAL METHODS

It is not trivial to investigate the hyperferroelectric properties since they require to determine the electric polarization, the electronic screening of electric fields, and the longitudinal optical (LO) phonon after the phonon interacts with macroscopic electric fields. To tackle these complex tasks, we use a combination of different computational methods to study the structural properties, electric polarization, dielectric susceptibility, and lattice vibrations of ZnO, all of which are needed in order to understand the hyperferroelectric properties of ZnO. These techniques are described below.

*Total-energy calculations and structure optimization:* The density functional theory (DFT) within the local density approximation (LDA)<sup>24,25</sup>, as implemented in Quantum Espresso<sup>26,27</sup>, is used to determine the total energy, atomic forces, and optimized structure. Norm-conserving pseudopotentials of Troullier-Martins type are used to mimic the effects of core electrons.<sup>28</sup> Semi-core states of Zn 3s and 3p are treated as the valence states to ensure better accuracy, and details of the atomic pseudopotentials were given in Ref.16. These pseudopotentials have been successfully used to determine the electromechanical  $d_{33}$  coefficient in ZnO under finite electric fields<sup>16</sup>, and to predict an interesting phase transition when ZnO is subjected to inplane tensile strains<sup>29</sup>.

*Modern theory of polarization:* Electric polarization in a solid consists of contributions from both ions and electrons. The ionic contribution ( $\vec{P}_{\text{ion}}$ ) can be calculated straightforwardly using point charges. The electronic contribution ( $\vec{P}_{\text{el}}$ ) is determined using the geometrical Berry-phase approach according to the modern theory of polarization<sup>30,31</sup>. More specifically, given Bloch wave functions  $|u_{n\vec{k}}\rangle$  at wave vector  $\vec{k}$ ,  $\vec{P}_{\text{el}}$  is calculated as  $\vec{P}_{\text{el}} = i \frac{2e}{(2\pi)^3} \int d\vec{k} \langle u_{n\vec{k}} | \nabla_{\vec{k}} | u_{n\vec{k}} \rangle = \frac{2e}{(2\pi)^3} \int d\vec{k}_{\perp} \phi(\vec{k}_{\perp})$  and

the polarization contribution  $\phi(\vec{k}_{\perp})$  at each  $\vec{k}_{\perp}$  is<sup>30,31</sup>

$$\begin{aligned} \phi(\vec{k}_{\perp}) &= i \sum_{n=1}^M \int d\vec{k}_{\parallel} \langle u_{n\vec{k}} | \frac{\partial}{\partial \vec{k}_{\parallel}} | u_{n\vec{k}} \rangle \\ &= \text{Im} \{ \ln \prod_j \det(\langle u_{n'\vec{k}_{\parallel}^j} | u_{n\vec{k}_{\parallel}^{j+1}} \rangle) \}, \end{aligned} \quad (1)$$

where  $\parallel$  and  $\perp$  mean, respectively, parallel and perpendicular to the direction of polarization, and  $M$  is the number of the occupied bands of an insulator. The electronic polarization  $\vec{P}_{\text{el}}$  can be further analyzed using the theory of polarization structure, which describes the relationship between phase  $\phi(\vec{k}_{\perp})$  and wave vector  $\vec{k}_{\perp}$ .<sup>32</sup>

*Density-functional linear response theory:* The density functional perturbation theory (DFPT)<sup>33-35</sup> is used to determine the effective charges, high-frequency dielectric constant  $\epsilon_{\infty}$  (namely the electronic contribution to the dielectric constant), phonon frequencies and eigenvectors of both non-centrosymmetric and centrosymmetric ZnO. In DFPT theory, the response  $|\Delta\psi_n\rangle$  of electron state to the potential deformation  $\Delta V(\vec{r})$  of bare ions caused by atomic vibration is determined by solving the Sternheimer equation<sup>33</sup>,

$$(H_{scf} - \epsilon_n) |\Delta\psi_n\rangle = -(\Delta V_{scf} - \Delta\epsilon_n) |\psi_n\rangle. \quad (2)$$

To determine whether ZnO retains its polar nature under OCBC with vanishing electric displacement ( $\vec{D}=0$ ), we need to determine the LO-phonon frequency and the structural instability of centrosymmetric ZnO at the Brillouin-zone center. For long-wavelength phonons with its wave vector  $\vec{q}$  approaching zero, the interatomic force-constant matrix can be separated into analytic and non-analytic parts  $C_{ij}^{\alpha\beta} = C_{ij}^{a,\alpha\beta} + C_{ij}^{na,\alpha\beta}$ , where  $i$  and  $j$  are atomic indices,  $\alpha$  and  $\beta$  are direction indices. The analytic part  $C_{ij}^{a,\alpha\beta}$  is computed from the DFPT perturbation theory,<sup>33-35</sup> and the nonanalytic part (due to interaction between lattice vibration and macroscopic electric field) is given as<sup>36</sup>  $C_{ij}^{na,\alpha\beta} = \frac{4\pi}{\Omega} e^2 \frac{(\vec{q} \cdot \mathbf{Z}_i^*)_{\alpha} (\vec{q} \cdot \mathbf{Z}_j^*)_{\beta}}{\vec{q} \cdot \epsilon_{\infty} \cdot \vec{q}}$ , where  $\mathbf{Z}_i^*$  is the Born effective-charge tensor of atom  $i$ . Since  $C^{na}$  is not diagonal, it often causes a strong mixing among different modes. This nonanalytic contribution leads to the difference in frequency between LO phonon and TO phonon. A rigorous definition of LO/TO splitting was given in Ref.37.

## III. RESULTS AND DISCUSSIONS

### A. Ground-state properties of polar ZnO

We first describe our first-principles results on the ground-state properties of the non-centrosymmetric (polar) ZnO, since polar ZnO is an important semiconductor of technological applications, and its properties are of interest to many readers. Ground state ZnO crystalizes in the wurtzite structure with lattice vectors

$\vec{a}_1 = a(\frac{1}{2}\vec{i} + \frac{\sqrt{3}}{2}\vec{j})$ ,  $\vec{a}_2 = a(-\frac{1}{2}\vec{i} + \frac{\sqrt{3}}{2}\vec{j})$ , and  $\vec{a}_3 = c\vec{k}$ , where  $a$  is the inplane lattice constant, and  $c$  is the out-of-plane lattice constant. Atoms inside a unit cell are shown in Fig.1, where four non-equivalent atoms are located at  $0\vec{a}_1 + 0\vec{a}_2 + 0\vec{a}_3$  (Zn1),  $0\vec{a}_1 + 0\vec{a}_2 + u\vec{a}_3$  (O1),  $\frac{1}{3}\vec{a}_1 + \frac{1}{3}\vec{a}_2 + \frac{1}{2}\vec{a}_3$  (Zn2), and  $\frac{1}{3}\vec{a}_1 + \frac{1}{3}\vec{a}_2 + (\frac{1}{2} + u)\vec{a}_3$  (O2).

We optimize both cell parameters ( $a$  and  $c/a$ ) and atomic positions (i.e., the internal parameter  $u$ ), and the optimal values of these quantities are given in Table I. After determining the optimized structure, we then compute, from DFPT linear-response calculations, the dielectric components  $\epsilon_{\infty}^{11}$  and  $\epsilon_{\infty}^{33}$  of high-frequency dielectric constant, and the Born effective charge  $Z_{33}^*$  of Zn and O atoms; the results are also shown in Table I.

Our theoretical values of  $a=3.250\text{\AA}$  and  $u=0.3791$  in Table I are in good agreement with the experimental measurement results of  $a=3.253\text{\AA}$  and  $u=0.382$ , respectively.<sup>38</sup> The Born effective charge  $Z_{33}^*=2.20$  of Zn in this study is also close to the experimental value<sup>39</sup> of 2.10 and another theoretical value<sup>40</sup> of 2.05. These indicate that our theoretical results are reasonably reliable.

According to the group theory<sup>41</sup>, the normal modes at the zone center of polar ZnO (with a wurtzite crystal structure and a point-group symmetry of  $C_{6v}$ ) are  $2A_1 \oplus 2B_1 \oplus 2E_1 \oplus 2E_2$ . Among them,  $A_1(\text{TO})$  and  $E_1(\text{TO})$  are polar modes,  $B_1$  is silent (i.e., both IR and Raman inactive), and  $E_2$  is non-polar and IR inactive (but Raman active). At the zone center, the acoustic  $A_1$  and  $E_1$  modes are trivial with zero frequencies and are thus not discussed further. For other nontrivial modes in polar ZnO, the computed phonon frequencies ( $\omega$ ), IR intensity, and phonon displacements ( $|d\rangle$ ) are given in Table II. Phonon displacement  $|d\rangle$  is related with the phonon eigenvector  $|e\rangle$  by  $d_{i\alpha}(l) = \frac{1}{\sqrt{M_i}} e_{i\alpha} e^{i\vec{q}\cdot\vec{R}_l}$ , where  $l$ ,  $i$ , and  $\alpha$  are respectively the indices for lattice sites, atoms inside a cell, and the Cartesian vibration directions, and  $\vec{q}$  is the phonon wave vector.

The theoretical phonon frequencies are comparable with the experimental measurements.<sup>42</sup> For instance, in Table II, the computed frequencies for  $A_1(\text{TO})$  ( $394\text{ cm}^{-1}$ ) and for  $E_1(\text{TO})$  ( $414\text{ cm}^{-1}$ ) are in good agreement with the experimental values which are  $380\text{ cm}^{-1}$  for  $A_1(\text{TO})$  and  $410\text{ cm}^{-1}$  for  $E_1(\text{TO})$ .<sup>42</sup> Furthermore, two notable observations can be seen in Table II: (i) The low-frequency phonons, e.g.,  $E_2$  at  $86\text{ cm}^{-1}$  and  $B_1$  at  $258\text{ cm}^{-1}$  have large contributions from Zn1 and Zn2 cation atoms, while the high-frequency phonons, e.g.,  $A_1(\text{TO})$  and  $E_1(\text{TO})$  have large contributions from O1 and O2 anion atoms. (ii)  $E_1(\text{LO})$  and  $E_1(\text{TO})$  have nearly identical phonon displacements in ZnO, showing that the LO and TO modes have one-to-one correspondence. This is in marked difference with the LO/TO phonons in ferroelectric perovskites  $\text{BaTiO}_3$  and  $\text{PbTiO}_3$ ; in the latter case it is known that LO and TO phonons do *not* have one-to-one correspondence<sup>43,44</sup>, and as a result, a rigorous definition of the LO/TO splitting need be carefully formulated.<sup>37</sup>

## B. Electric equations of state: the E- $\lambda$ and D- $\lambda$ relations

To find whether ZnO is HyFE, we need to determine whether ZnO can retain ferroelectric polarization with nonzero atomic off-center displacements under OCBC (i.e., under the condition in which electric displacement  $\vec{D}$  vanishes along the polar direction). We therefore intend to determine the electric equation of state, which is the relationship between electric displacement and polarization. We use two atomic configurations: one is the ground-state configuration of polar ZnO where the optimal atomic positions are denoted as  $\vec{r}_i^{\text{opt}}$ , and the other is the centrosymmetric configuration of nonpolar ZnO where atoms are located at high-symmetry nonpolar positions (to be denoted as  $\vec{r}_i^c$ ). We then construct the intermediate configurations, controlled by parameter  $\lambda$  as  $\vec{r}_i(\lambda) = \vec{r}_i^c + \lambda(\vec{r}_i^{\text{opt}} - \vec{r}_i^c)$ . Each  $\lambda$  yields a different atomic configuration with different polarization. Obviously the nonpolar configuration and the optimal polar configuration are just two special cases among all possible  $\vec{r}_i(\lambda)$  configurations: the former corresponds to  $\lambda = 0$  while the latter corresponds to  $\lambda = 1$ .

We begin with the free energy  $F(\lambda)$  when ZnO is under an electric field  $E$ , which is applied along the polar direction.  $F(\lambda)$  is defined as<sup>45</sup>

$$F(\lambda) = U(\lambda) - \Omega(\lambda) \left[ P(\lambda)E + \frac{1}{2}\epsilon_0\chi_{\infty}(\lambda)E^2 \right], \quad (3)$$

where  $U(\lambda)$ ,  $P(\lambda)$ ,  $\chi_{\infty}(\lambda)$ , and  $\Omega(\lambda)$  are respectively the DFT total energy per unit cell, the electric polarization, the diagonal component  $\chi_{\infty}^{33}$  of high-frequency dielectric permittivity along the polar direction, and the unit-cell volume of ZnO when the bulk solid is at configuration  $\lambda$ .  $\epsilon_0$  is the dielectric constant of free space. Since the electric field is applied along the polar direction of ZnO, the vector signs are dropped in Eq.(3). The method of building free energy has also been used in the interface design for enhanced ferroelectricity<sup>46</sup>.

Equation (3) is essentially a second-order Tylor expansion of  $F(\lambda)$  as a function of  $E$  at the configuration  $\lambda$ , with the expansion coefficients  $U(\lambda)$ ,  $P(\lambda)$ , and  $\chi_{\infty}(\lambda)$  corresponding to the quantities at zero macroscopic field. Therefore  $U(\lambda)$ ,  $P(\lambda)$ , and  $\chi_{\infty}(\lambda)$  need be computed under the short-circuit boundary condition (SCBC) with  $E=0$ . On the other hand, since the macroscopic field  $E$  in Eq.(3) may be either zero or nonzero, the free energy  $F(\lambda)$  in Eq.(3) can thus describe the situations of either SCBC, or OCBC, or circumstances other than SCBC or OCBC.

For a given  $E$  field, the optimal  $\lambda$  should satisfy  $\frac{\partial F}{\partial \lambda} = 0$ , namely,

$$\frac{\partial U(\lambda)}{\partial \lambda} - \left[ \frac{\partial(\Omega P)}{\partial \lambda} E + \frac{1}{2}\epsilon_0 \frac{\partial(\Omega\chi_{\infty})}{\partial \lambda} E^2 \right] = 0. \quad (4)$$

Here, it worths mentioning that knowing how  $U(\lambda)$ ,  $P(\lambda)$ , and  $\chi_{\infty}(\lambda)$  depend on  $\lambda$  (which can be computed

from the DFT and DFPT calculations), it is straightforward to determine using Eq.(4) the  $E \sim \lambda$  relation. In contrast, it is generally not a good idea to determine the *inverse*  $\lambda \sim E$  relation, which actually is not needed. Furthermore, Eq.(4) tells that the  $E$  field is determined only by the derivatives  $\frac{\partial U(\lambda)}{\partial \lambda}$ ,  $\frac{\partial(\Omega P)}{\partial \lambda}$ , and  $\frac{\partial(\Omega \chi_\infty)}{\partial \lambda}$ , rather than by the magnitudes of  $U$  and  $P$ .

To obtain the  $D \sim \lambda$  relation, we determine using Eq.(3) the electric polarization as  $P_{tot} = -\frac{1}{\Omega} \frac{\partial F}{\partial E} = P(\lambda) + \epsilon_0 \chi_\infty(\lambda) E$ , where the first term accounts for the fact that the electric field will cause ions to displace, and the second term account for the effect that the electric field will also polarize the wave functions of valence electrons. The electric displacement  $D$  then becomes

$$D = \epsilon_0 E + P_{tot} = \epsilon_0 [1 + \chi_\infty(\lambda)] E + P(\lambda). \quad (5)$$

When combined with the  $E \sim \lambda$  relation obtained from Eq.(4), Eq.(5) leads to the  $D \sim \lambda$  relation. Using this  $D \sim \lambda$  relation, one can examine whether the atomic off-center displacement  $\lambda$  vanishes under OCBC ( $D=0$ ), to find out whether ZnO is HyFE. If polar displacement exists (i.e.,  $\lambda \neq 0$ ) when  $D=0$ , then the solid is a HyFE.

In principle, the free energy in open-circuit (or short-circuit) boundary condition can be obtained using the fixed- $E$  or fixed- $D$  methods<sup>45</sup>. However, the computation will be intensive for the following reasons. (i) The electric field in the fixed- $E$  or fixed- $D$  methods couples the single-particle states at different electron wave vectors  $\vec{k}$ , and the Berry-phase calculation of polarization must be inside the charge self-consistent process (not as a post-process). Both make the computation time-consuming. (ii) Atomic geometry need be optimized for each electric field, which further increases computation. In contrast, the current approach used here has several advantages. First, all calculations are performed at zero macroscopic field using common DFT methods, and the approach can thus be widely applied. Further, the approach offers important physics insight as demonstrated analytically in this paper. We should also mention that the nonlinear effect is largely included in Eq.(3). Since  $\lambda$  depends implicitly on the  $E$  field as shown in Eq.(4), polarization  $P(\lambda)$  and high-frequency dielectric susceptibility  $\chi_\infty(\lambda)$  thus also depend on  $E$ . Therefore, the coupling term  $\Omega(\lambda) [P(\lambda)E + \frac{1}{2}\epsilon_0 \chi_\infty(\lambda) E^2]$  in Eq.(3) includes the nonlinear effect.

Our calculated  $U \sim \lambda$  relation (obtained from DFT structural optimization and total-energy calculations), and the  $P \sim \lambda$  relation (obtained from the Berry phase calculations using the modern theory of polarization), are shown in Fig.2, while the calculated  $\epsilon_\infty \sim \lambda$  relation (obtained from the DFPT linear-response calculations) is depicted in the inset of Fig.2.

From Fig.2, we see that: (i) Under the short-circuit boundary condition, the  $U \sim \lambda$  curve shows that the non-polar ZnO (at  $\lambda=0$ ) is not stable, and polar ZnO (at  $\lambda=1$ ) is stable as it should be. When  $\lambda$  is increased to be larger than 1,  $U$  increases sharply, which is energetically less favorable. The depth of potential well

$\Delta U = U(\lambda = 1) - U(\lambda = 0)$  is -0.609 eV. This  $\Delta U$  is in fact comparable to the well depths (typically ranging from -0.20 to -0.80 eV) in the recently-discovered ABC-type ferroelectrics<sup>47</sup>. (ii) The polarization  $P$  depends on  $\lambda$  in a linear fashion, increasing from zero at  $\lambda=0$  to 0.844 C/m<sup>2</sup> at  $\lambda=1$ . In other words,  $P = 0.844\lambda$ , and  $\lambda$  is thus a direct measure of the magnitude of polarization by being proportional to the latter. (iii) High-frequency  $\epsilon_\infty(\lambda)$  in the inset of Fig.2 shows a non-monotonous dependence on  $\lambda$ , increasing from  $\epsilon_\infty=4.37$  at  $\lambda=0$  to  $\epsilon_\infty=5.09$  at  $\lambda=1$ , and then starting to decrease at  $\lambda \geq 1$ .

The  $E \sim \lambda$  relation, determined from Eq.(4), and the  $D \sim \lambda$  relation, determined from Eq.(5), are shown in Fig.3. It worths pointing out that the  $E \sim \lambda$  and  $D \sim \lambda$  curves themselves are of considerable significance in terms of understanding the electrical properties, in addition to determining whether a solid is HyFE. In fact, electric  $D$  displacement was shown to be a fundamental variable in electronic-structure calculations.<sup>45,48</sup> Several marked observations can be made in Fig.3.

First, and interestingly, we see in Fig.3 that the  $E \sim \lambda$  curve has three roots at  $\lambda = 0$  and  $\lambda = \pm 1$ . This does not occur by accident, and can be intuitively explained as follows. At the above three  $\lambda$  values, energy  $U$  is either a minimum or a saddle point, i.e.,  $\frac{\partial U(\lambda)}{\partial \lambda} = 0$ . Meanwhile, it can be easily seen from Eq.(4) that, when  $\frac{\partial U(\lambda)}{\partial \lambda} = 0$ , Eq.(4) has a solution of  $E = 0$ , which explains why  $\lambda = 0$  and  $\lambda = \pm 1$  must be the roots of the  $E \sim \lambda$  curve.

However, the  $D \sim \lambda$  curve in Fig.3 reveals that it has only one root at  $\lambda=0$ , showing that, only when  $\lambda$  is zero, electric displacement  $D$  vanishes. Since  $\lambda=0$  corresponds to a nonpolar phase, the  $D \sim \lambda$  curve in Fig.3 thus demonstrates that ZnO is nonpolar under the open-circuit boundary condition  $D = 0$ , or in other words, ZnO is not HyFE. In order to be HyFE, the solid needs to exhibit a  $D \sim \lambda$  relation as shown in the inset of Fig.3, where the curve has three roots at A, B, and B'. At B and B',  $\lambda$  is nonzero.

It is important to understand why the  $D \sim \lambda$  curve of ZnO in Fig.3 does not possess a nonzero root. We recognize from the  $E \sim \lambda$  curve in Fig.3 that the electric field  $E$  at  $\lambda=0.6$  is negative and large in magnitude. Since  $D$  is directly related to  $E$ , it raises an interesting question, that is, why the  $D$  value near  $\lambda=0.6$  is not negative, which may otherwise lead to a nonzero root for  $D$ . The question can be answered by Eq.(5). Although the first term in Eq.(5) is negative, the  $P(\lambda)$  term at  $\lambda=0.6$  is nevertheless positive and dominates, which results in a positive  $D$ . We thus see that a large spontaneous polarization could be detrimental to the occurrence of hyperferroelectricity. This result is, interestingly, consistent with the general guideline proposed in Ref.9 that a HyFE needs to have a deep double-potential well and a small polarization.

### C. Free energy under OCBC

An alternative (and efficient) approach to investigate whether a solid is HyFE is to determine the free energy under the open-circuit boundary condition. When  $D$  vanishes, one obtains using Eq.(5) that

$$E = -\frac{P(\lambda)}{\epsilon_0 [1 + \chi_\infty(\lambda)]} . \quad (6)$$

By substituting the above expression into Eq.(3), the free energy  $F$  under the  $D=0$  condition can be determined as

$$F(\lambda) = U(\lambda) - \Omega(\lambda) \left\{ -\frac{P^2(\lambda)}{\epsilon_0 [1 + \chi_\infty(\lambda)]} + \frac{1}{2} \chi_\infty(\lambda) \frac{P^2(\lambda)}{\epsilon_0 [1 + \chi_\infty(\lambda)]^2} \right\} . \quad (7)$$

One distinctive feature of this free-energy approach is that there is no need to determine the  $E \sim \lambda$  and  $D \sim \lambda$  relations (which are often less accurate since they require numerical derivatives). Instead, knowing the  $U(\lambda)$ ,  $P(\lambda)$ ,  $\chi_\infty(\lambda)$  curves as computed in Fig.2, we can directly calculate using Eq.(7) the free energy as a function of  $\lambda$ .

The free energy for ZnO under OCBC is depicted in Fig.4. Comparing the  $U(\lambda)$  curve in Fig.2 and the  $F(\lambda)$  curve in Fig.4, we see two critical differences: (i) Although the  $U(\lambda)$  curve has a minimum at  $\lambda=1$  (which forms one of the two minima of the double-potential well), the  $F(\lambda)$  curve nevertheless has only one minimum at  $\lambda=0$ . (ii)  $U$  is unstable at  $\lambda=0$  by being a saddle point, but  $F$  is stable at  $\lambda=0$ . Fig.4 thus reveals that, under OCBC, the free energy of ZnO is stable only at the *nonpolar* phase with  $\lambda=0$ . In other words, ZnO is nonpolar under OCBC. Therefore ZnO is not HyFE, which is consistent with the results obtained from the electric equation of state in the previous section.

From the point of view of free energy, the reason that ZnO is not HyFE can be understood as follows. Under OCBC, if ZnO were polar with nonzero polarization, then a nonzero depolarization  $E$  field will be generated according to Eq.(6). This strong and non-vanishing depolarization field increases the contribution of the second term in Eq.(7) to the free energy, which ultimately eliminates the polarization.

The theoretical finding that ZnO is not HyFE is consistent with available experimental observation. In experiment, polar surface of ZnO was found to be unstable, and it undergoes surface reconstruction.<sup>49</sup> The observation is in agreement with our result that ZnO is not polar under OCBC. Furthermore, according to our theory, the instability of ZnO polar surface is caused by the existence of strong depolarization field.

### D. LO phonon in ZnO

When a hyperferroelectric solid is in its (unstable) centrosymmetric phase, its *longitudinal*-optic (LO) phonon

should exhibit an imaginary frequency at the zone center<sup>1,9,10</sup>, which manifests the fact that ferroelectric instability persists despite the existence of depolarizing field. Here it is worth pointing out that, when a solid is in the centrosymmetric phase, whereas a soft *transverse*-optic (TO) phonon at the zone center is quite common and indicates the existence of ferroelectric instability<sup>7</sup>, a soft LO phonon at the zone center is rare, which explains why HyFE is unique and special.

To determine whether ZnO possesses a soft LO phonon, we have computed the TO and LO frequencies of the centrosymmetric (nonpolar) ZnO, using the DFPT linear response theory. We find  $\omega_{\text{TO}}=243i \text{ cm}^{-1}$ , showing that nonpolar ZnO is unstable with an imaginary  $\omega_{\text{TO}}$  frequency under the short-circuit boundary condition of  $E=0$ , as it should. Meanwhile, we find  $\omega_{\text{LO}}=255 \text{ cm}^{-1}$ , revealing that nonpolar ZnO is stable with a large and positive  $\omega_{\text{LO}}$  frequency under the open-circuit boundary condition of  $D=0$ . This reveals that ZnO is not HyFE.

It is interesting to go one step further and explore why ZnO is not HyFE although it has a similar wurtzite structure as the ABC-type semiconductor LiZnAs; LiZnAs on the other hand was discovered to be HyFE<sup>1</sup>. We find that it may be attributed to the small high-frequency dielectric constant  $\epsilon_\infty$  in ZnO. To demonstrate this, we examine nonpolar ZnO and numerically change its  $\epsilon_\infty$  value, and then compute the non-analytic part  $C_{ij}^{na,\alpha\beta}$  of the dynamical matrix as well as the frequency of LO phonon. The obtained frequency squared,  $\omega_{\text{LO}}^2$ , of the LO-phonon is shown in Fig.5 as a function of  $\epsilon_\infty$ . The DFT-computed value of  $\epsilon_\infty$  is 4.37 for nonpolar ZnO. Fig.5 shows that, when  $\epsilon_\infty$  is artificially increased from 4.37,  $\omega_{\text{LO}}^2$  decreases sharply. As  $\epsilon_\infty$  is increased to a critical value  $\epsilon_\infty^c=9.12$ ,  $\omega_{\text{LO}}^2$  becomes negative and ZnO becomes a HyFE. The result reveals that a moderate increase in  $\epsilon_\infty$  will turn ZnO into a HyFE, signaling that small  $\epsilon_\infty$  value is indeed responsible for ZnO to be non-HyFE. Interestingly, this discovery is consistent with LiZnAs and other ABC-type HyFE semiconductors, which all have a fairly large  $\epsilon_\infty$  on the order of  $\sim 15$ .<sup>1</sup>

To further confirm that a larger  $\epsilon_\infty$  value will indeed turn ZnO into a HyFE, we change the  $\epsilon_\infty$  value of nonpolar ZnO to 10.37 (which is larger than the critical value of  $\epsilon_\infty^c=9.12$ ), and calculate using Eq.(7) the free energy under OCBC as a function of  $\lambda$ . The result is depicted in the inset of Fig.4, showing that the free energy now exhibits *double* minima at nonzero  $\lambda = \pm 0.18$ . Therefore, ZnO indeed becomes a HyFE when  $\epsilon_\infty$  is increased. The fact that ZnO can be turned into HyFE also suggests that, compared to LiZnAs, wurtzite semiconductors may become hyperferroelectric without Li.

There are two possible routes in experiments to change the  $\epsilon_\infty$  value in ZnO. One is by biaxial inplane strain<sup>29</sup>, and the other is by doping. Both routes will alter the band gap of ZnO and thus the high-frequency electronic contribution to the dielectric constant.

Our theoretical study also provides a unified scheme linking different explanations for the origin of

hyperferroelectricity.<sup>1,9–11</sup> From the point of view of LO phonon, a large high-frequency dielectric  $\epsilon_\infty$  constant shall reduce the LO/TO splitting and give rise to a soft LO phonon, which is consistent with the explanation of Garrity *et al.* that HyFE is caused by small LO/TO splitting.<sup>1</sup> Meanwhile, large  $\epsilon_\infty$  constant will also lead to meta-screening, which is in accord with the explanation in Ref.11. From the point of view of the free energy under OCBC, a small spontaneous polarization, a large high-frequency dielectric  $\chi_\infty$  susceptibility, and a deep potential well all favor the emergence of double minima in free energy [see Eq.(7)], which is consistent with the explanation of Ref.9. Furthermore, a large dielectric  $\epsilon_\infty$  constant will lead to a strong screening of the long-range interaction and make the short-range interaction become prominent in causing hyperferroelectricity, which is in line with the explanation in Ref.10.

To confirm that our theory in Eq.(7) also works for other materials, we apply it to LiBeSb, one of the hyperferroelectrics in Ref.1. As shown in the inset of Fig.4, in order for a solid to be hyperferroelectric, the free energy  $F$  in Eq.(7) should have double minima. In other words, the  $F \sim \lambda$  curve should have a *negative* curvature near  $\lambda = 0$ . By using the computation data available in Ref.1, we find that the  $F \sim \lambda$  relation for LiBeSb is  $F = -0.1686\lambda^2$  eV per unit cell, showing that the curvature is indeed negative. Therefore, LiBeSb is a hyperferroelectric according to Eq.(7), and our theory is thus general and works for other materials.

#### IV. SUMMARY

Hyperferroelectricity is an interesting phenomenon, and understanding whether a solid is HyFE is a topic of importance. We have described three approaches to investigate the hyperferroelectric properties of ZnO, which include (a) determining the electric equation of state, (b) calculating the free energy under OCBC, and (c) determining the properties of LO phonon. The current study also provides a unified scheme linking different explanations for the origin of hyperferroelectricity. Our specific findings are summarized in the following.

(i) The  $E \sim \lambda$  relation is shown to be determined only by the derivatives  $\frac{\partial U(\lambda)}{\partial \lambda}$ ,  $\frac{\partial(\Omega P)}{\partial \lambda}$ , and  $\frac{\partial(\Omega \chi_\infty)}{\partial \lambda}$ , as revealed in Eq.(4). For a ferroelectric solid, we find that the  $E \sim \lambda$  curve must have three roots at  $\lambda = 0$  and  $\lambda = \pm 1$ .

When ZnO is under the *short-circuit* boundary condition, the depth  $\Delta U$  of the double-potential well is found to be 0.609 eV, which is comparable to those in ABC-type semiconductor ferroelectrics<sup>47</sup>. The polarization in ZnO is shown to be directly proportional to  $\lambda$  as  $P = 0.844\lambda$  C/m<sup>2</sup>.

On the other hand, when ZnO is under the *open-circuit* boundary condition, we find that its  $D \sim \lambda$  curve exhibits only one root at  $\lambda = 0$ , showing that ZnO possesses no polarization when  $D=0$ . ZnO is thus not a HyFE. The absence of nonzero root in the  $D \sim \lambda$  curve of ZnO can be attributed to the large spontaneous polarization, namely the second term in Eq.(5) is detrimentally too large.

(ii) To predict whether a solid is HyFE, we find that an alternative (and more effective) approach is to calculate, directly using Eq.(7), the free energy under OCBC, which bypasses the determination of the  $D \sim \lambda$  relation. Using this approach, we reveal that the free energy of ZnO under OCBC is most stable at  $\lambda=0$ , and ZnO is thus not polar under OCBC, which is consistent with the result obtained from the electric equation of state.

(iii) For centrosymmetric ZnO, our linear response calculations yield a soft TO mode with frequency  $\omega_{\text{TO}}=243i$  cm<sup>-1</sup>, which shows that ZnO has a polar instability under the short-circuit boundary condition. But, the LO frequency  $\omega_{\text{LO}}=255$  cm<sup>-1</sup> does not have imaginary frequency and is not soft, revealing that ZnO is stable (and thus not a HyFE) under the open-circuit boundary condition.

Furthermore, that ZnO is not a HyFE originates from its small high-frequency dielectric constant. We show that, when  $\epsilon_\infty$  of ZnO is increased beyond a critical value  $\epsilon_\infty^c=9.12$ , ZnO indeed becomes a HyFE by possessing a soft LO mode (as shown in Fig.5) as well as double minima of free energy (as depicted in the inset of Fig.4).

Considering that hyperferroelectricity is still at the beginning and remains not adequately understood, we hope that our study will stimulate more theoretical and experimental work on this interesting phenomenon.

#### Acknowledgments

This work was partially supported by the Office of Naval Research. Computations were performed on the computing facilities provided by the Arkansas High-Performance Computing Center, supported by NSF.

<sup>1</sup> K.F. Garrity, K.M. Rabe, and D. Vanderbilt, Phys. Rev. Lett. **112**, 127601 (2014).

<sup>2</sup> N.A. Benedek and M. Stengel, Physics **7**, 32 (2014).

<sup>3</sup> C.J. Fennie and K.M. Rabe, Phys. Rev. B **72**, 100103 (2005).

<sup>4</sup> E. Bousquet, M. Dawber, N. Stucki, C. Lichtensteiger, P. Hermet, S. Gariglio, J.-M. Triscone, and P. Ghosez, Nature (London) **452**, 732 (2008).

<sup>5</sup> N.A. Benedek and C.J. Fennie, Phys. Rev. Lett. **106**, 107204 (2011).

<sup>6</sup> M. Stengel, C.J. Fennie, and P. Ghosez, Phys. Rev. B **86**, 094112 (2012).

<sup>7</sup> M.E. Lines and A.M. Glass, *Principles and Applications of Ferroelectrics and Related Materials* (Clarendon Press, Oxford, 1977).

<sup>8</sup> M. Dawber, K.M. Rabe, and J.F. Scott, Rev. Mod. Phys.

- 77**, 1083 (2005).
- <sup>9</sup> H. Fu, J. Appl. Phys. **116**, 164104 (2014).
  - <sup>10</sup> P. Li, X. Ren, G.-C. Guo, and L. He, Sci. Rep. **6**, 34085 (2016).
  - <sup>11</sup> H.J. Zhao, A. Filippetti, C. Escorihuela-Sayalero, P. Delugas, E. Canadell, L. Bellaiche, V. Fiorentini, and J. Iniguez, Phys. Rev. B **97**, 054107 (2018).
  - <sup>12</sup> S. Liu and R.E. Cohen, Phys. Rev. Lett. **119**, 207601 (2017).
  - <sup>13</sup> Z.W. Pan, Z.R. Dai, and Z.L. Wang, Science **291**, 1947 (2001).
  - <sup>14</sup> P.X. Gao, Y. Ding, W. Mai, W.L. Hughes, C. Lao, and Z. L. Wang, Science **309**, 1700 (2005).
  - <sup>15</sup> N.A. Hill and U. Waghmare, Phys. Rev. B **62**, 8802 (2000).
  - <sup>16</sup> D. Karanth and H. Fu, Phys. Rev. B **72**, 064116 (2005).
  - <sup>17</sup> H. Fu and L. Bellaiche, Phys. Rev. Lett. **91**, 057601 (2003).
  - <sup>18</sup> S.-E. Park and T.R. Shrout, J. Appl. Phys. **82**, 1804 (1997).
  - <sup>19</sup> A. Garcia and D. Vanderbilt, Appl. Phys. Lett. **72**, 2981 (1998).
  - <sup>20</sup> H. Fu and R.E. Cohen, Nature **403**, 281 (2000).
  - <sup>21</sup> F.A. Ponce and D.P. Bour, Nature (London) **386**, 351 (1997).
  - <sup>22</sup> C.H. Park, S.B. Zhang, and S.-H. Wei, Phys. Rev. B **66**, 073202 (2002).
  - <sup>23</sup> S. Limpijumnong, S.B. Zhang, S.-H. Wei, and C.H. Park, Phys. Rev. Lett. **92**, 155504 (2004).
  - <sup>24</sup> P. Hohenberg and W. Kohn, Phys. Rev. **136**, B864 (1964).
  - <sup>25</sup> W. Kohn and L.J. Sham, Phys. Rev. **140**, A1133 (1965).
  - <sup>26</sup> P. Giannozzi *et al.*, J. Phys. C **21**, 395502 (2009).
  - <sup>27</sup> <http://www.quantum-espresso.org>.
  - <sup>28</sup> N. Troullier and J. L. Martins, Phys. Rev. B **43**, 1993 (1991).
  - <sup>29</sup> Z. Alahmed and H. Fu, Phys. Rev. B **77**, 045213 (2008).
  - <sup>30</sup> R.D. King-Smith and D. Vanderbilt, Phys. Rev. B **47**, 1651 (1993).
  - <sup>31</sup> R. Resta, Rev. Mod. Phys. **66**, 899 (1994).
  - <sup>32</sup> Y. Yao and H. Fu, Phys. Rev. B **79**, 014103 (2009).
  - <sup>33</sup> S. Baroni, S. de Gironcoli, A. Dal Corso, and P. Giannozzi, Rev. Mod. Phys. **73**, 515 (2001).
  - <sup>34</sup> S. Baroni, P. Giannozzi, and A. Testa, Phys. Rev. Lett. **58**, 1861 (1987).
  - <sup>35</sup> X. Gonze, Phys. Rev. A **52**, 1096 (1995).
  - <sup>36</sup> X. Gonze and C. Lee, Phys. Rev. B **55**, 10355 (1997).
  - <sup>37</sup> A. Raeliarijaona and H. Fu, Phys. Rev. B **92**, 094303 (2015).
  - <sup>38</sup> H. Karzel, W. Potzel, M. Kofferlein, W. Schiessl, M. Steiner, U. Hiller, G.M. Kalvius, D.W. Mitchell, T.P. Das, P. Blaha, K. Schwarz, and M.P. Pasternak, Phys. Rev. B **53**, 11425 (1996).
  - <sup>39</sup> K.-H. Hellwege and O. Madelung, *Numerical Data and Functional Relationships in Science and Technology*, Landolt-Bornstein, New Series, Group III, Vol.17a (Springer, New York, 1982); Vol.22a (Springer, New York, 1982).
  - <sup>40</sup> A. Dal Corso, M. Posternak, R. Resta, and A. Baldereschi, Phys. Rev. B **50**, 10715 (1994).
  - <sup>41</sup> M.S. Dresselhaus, G. Dresselhaus, and A. Jorio, *Group Theory* (Springer-Verlag, Berlin, 2010).
  - <sup>42</sup> J. Serrano, F.J. Manjon, A.H. Romero, A. Ivanov, M. Cardona, R. Lauck, A. Bosak, and M. Krisch, Phys. Rev. B **81**, 174304 (2010).
  - <sup>43</sup> W. Zhong, R.D. King-Smith, and D. Vanderbilt, Phys. Rev. Lett. **72**, 3618 (1994).
  - <sup>44</sup> D. M. Eagles, J. Phys. Chem. Solids **25**, 1243 (1964).
  - <sup>45</sup> M. Stengel, N.A. Spaldin, and D. Vanderbilt, Nat. Phys. **5**, 304 (2009).
  - <sup>46</sup> H. Wang, J. Wen, D.J. Miller, Q. Zhou, M. Chen, H.N. Lee, K.M. Rabe, and X. Wu, Phys. Rev. X **6**, 011027 (2016).
  - <sup>47</sup> J.W. Bennett, K.F. Garrity, K.M. Rabe, and D. Vanderbilt, Phys. Rev. Lett. **109**, 167602 (2012).
  - <sup>48</sup> M. Stengel, D. Vanderbilt, and N. Spaldin, Nat. Mat. **8**, 392 (2009).
  - <sup>49</sup> O. Dulub, U. Diebold, and G. Kresse, Phys. Rev. Lett. **90**, 016102 (2003).



TABLE I: Theoretical quantities (the second column) obtained from our first-principles calculations for ground-state polar ZnO. The available experimental results are given in the third column for comparison.

Quantities	Present work	Experiments
$a$ (Å)	3.250	3.253 (Ref.38)
$c/a$	1.613	1.603 (Ref.39)
$u$	0.3791	0.382 (Ref.38)
$\epsilon_{\infty}^{11}$	4.73	
$\epsilon_{\infty}^{33}$	5.09	
$Z_{33}^*$ (Zn)	2.20	2.10 (Ref.39)
$Z_{33}^*$ (O)	-2.20	-2.10

TABLE II: DFPT-calculated phonon frequencies (2nd column), IR intensity (3rd column), and phonon displacements (4th column) of polar ZnO at the zone center. The experimental results on phonon frequencies are given in the parenthesis in the second column for comparison (Ref.42). In the fourth column, the vibration direction, i.e., the polarization direction of phonon, is given as the subscript, and the four components in  $|d\rangle$  correspond to the displacements of Zn1, O1, Zn2, O2 atoms in sequence.

Phonon	$\omega$ (cm $^{-1}$ )	IR	Displacement $ d\rangle$
E <sub>2</sub>	86	0.0	(-0.536,0.461,0.536,-0.461) <sub>x</sub>
B <sub>1</sub>	258	0.0	(-0.677,-0.204,0.677,0.204) <sub>z</sub>
A <sub>1</sub> (TO)	394 (380)	17.3	(0.169,-0.687,0.168,-0.686) <sub>z</sub>
E <sub>1</sub> (TO)	414 (410)	15.8	(-0.168,0.687,-0.168,0.687) <sub>x</sub>
E <sub>2</sub>	445 (438)	0.0	(-0.146,-0.692,0.146,0.692) <sub>x</sub>
B <sub>1</sub>	547	0.0	(0.052,-0.705,-0.052,0.705) <sub>z</sub>
A <sub>1</sub> (LO)	554	17.3	(-0.168,0.687,-0.168,0.687) <sub>z</sub>
E <sub>1</sub> (LO)	566	15.8	(-0.168,0.687,-0.168,0.687) <sub>x</sub>

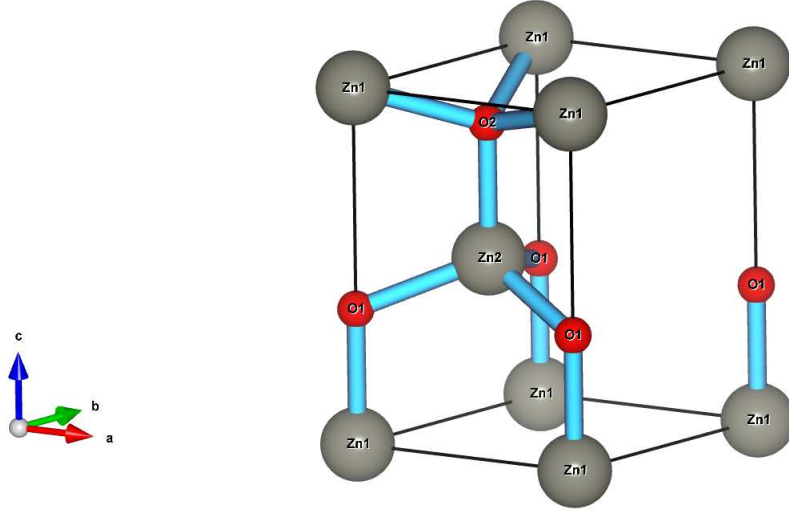


FIG. 1: One unit cell of wurtzite ZnO crystal, where non-equivalent atoms are labelled as Zn1, Zn2, O1, O2. The  $\vec{a}_1$ ,  $\vec{a}_2$ ,  $\vec{a}_3$  lattice vectors point at the  $\vec{a}$ ,  $\vec{b}$ ,  $\vec{c}$  directions in this figure.

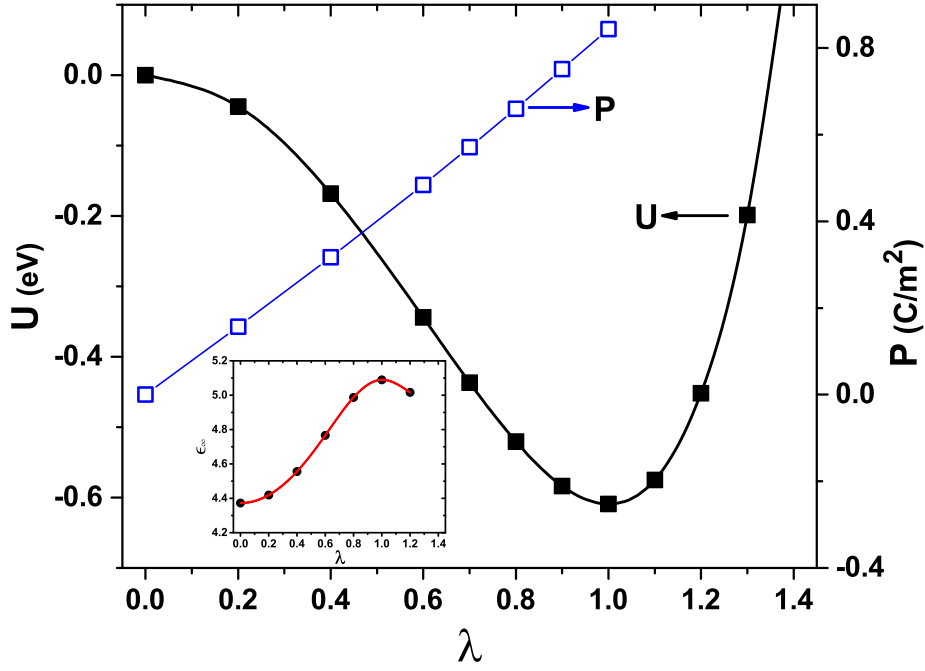


FIG. 2: The total energy  $U$  (solid squares, using the left vertical axis) and polarization  $P$  (empty squares, using the right vertical axis) as a function of  $\lambda$ . Inset shows the high-frequency dielectric constant  $\epsilon_\infty$  (solid dots) at different  $\lambda$ . These quantities ( $U$ ,  $P$ , and  $\epsilon_\infty$ ) are calculated under SCBC. The total energy  $U(\lambda = 0)$  at  $\lambda=0$  is chosen to be the zero reference energy. Symbols are the direct DFT calculation results, and lines are fitting curves using cubic splines.

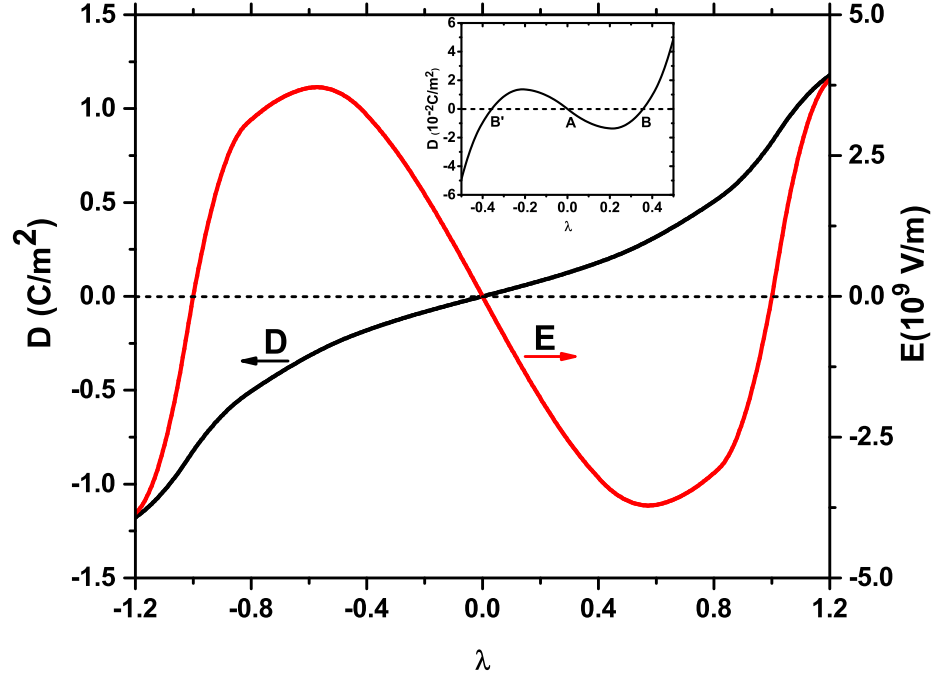


FIG. 3: (color online) The  $D \sim \lambda$  relation (black curve, using the left vertical axis) and the  $E \sim \lambda$  relation (red curve, using the right vertical axis) for ZnO. Inset shows a schematic  $D \sim \lambda$  relation which a HyFE should exhibit.

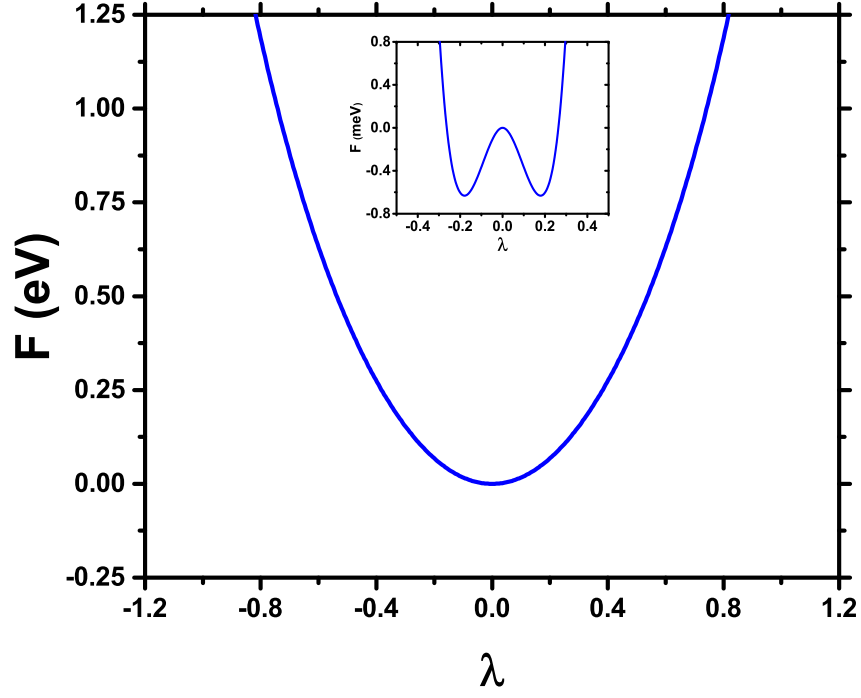


FIG. 4: Free energy  $F(\lambda)$  of ZnO under an open-circuit boundary condition as a function of  $\lambda$ . Inset shows the free energy of ZnO under an open-circuit boundary condition when the dielectric constant of centrosymmetric ZnO is increased to  $\epsilon_{\infty} = 10.37$ .

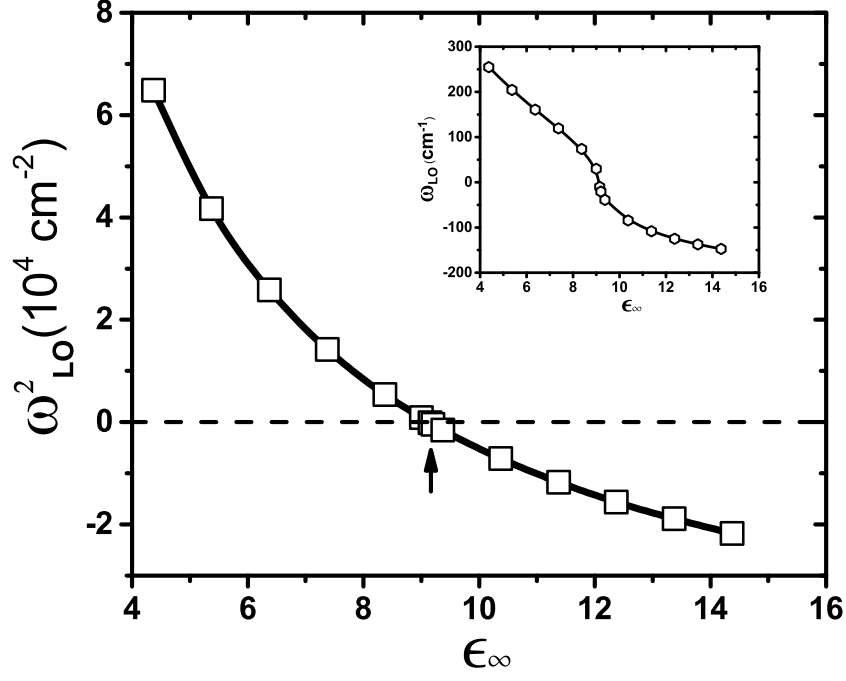


FIG. 5: Frequency squared ( $\omega_{LO}^2$ ) of the LO phonon in centrosymmetric ZnO as a function of  $\epsilon_\infty$ . Arrow marks the critical  $\epsilon_\infty$  value at which  $\omega_{LO}^2$  becomes negative. Inset shows how the LO frequency ( $\omega_{LO}$ ) varies with  $\epsilon_\infty$ . In the inset, imaginary frequencies are plotted as negative values.